Journal of Electronic Research and Application, 2024, Volume 8, Issue 3
http://ojs.bbwpublisher.com/index.php/JERA
ISSN Online: 2208-3510
ISSN Print: 2208-3502

Design of IoT-based Volatile Organic Compounds Monitoring System

Bo Wang, Minghao Ma*

School of Mechanical and Electrical Engineering, Shaanxi University of Science and Technology, Xi'an 710021, Shaanxi Province, China

Corresponding author: Minghao Ma, 18049134130@163.com

Abstract: Volatile organic compounds (VOC) gas detection devices based on semiconductor sensors have become a common method due to their low cost, simple principle, and small size. However, with the continuous development of materials science, various new materials have been applied in the fabrication of gas sensors, but these new materials have more stringent requirements for operating temperature, which cannot be met by existing sensor modules on the market. Therefore, this paper proposes a temperature-adjustable sensor module and designs an environmental monitoring system based on the STM32F103RET6 microprocessor. This system primarily utilizes multiple semiconductor gas sensors to monitor and record the concentrations of various harmful gases in different environments. It can also monitor real-time temperature, humidity, and latitude and longitude in the current environment, and upload the data to the Internet of Things via 4G communication. This system has the advantages of small size, portability, and low cost. Experimental results show that the sensor module can achieve precise control of operating temperature to a certain extent, with an average temperature error of approximately 3%. The monitoring system demonstrates a certain level of accuracy in detecting target gases and can promptly upload the data to a cloud platform for storage and processing. A comparison with professional testing equipment shows that the sensitivity curves of each sensor exhibit similarity. This study provides engineering and technical references for the application of VOC gas sensors.

Keywords: Sensors; IoT; Environmental monitoring; VOC sensor; STM32F103RET6

Online publication: June 13, 2024

1. Introduction

With the continuous development of society, various new types of organic materials have emerged and are increasingly applied in people's daily lives. However, the production of these new organic materials often accompanies the emission of volatile organic compounds (VOCs) that are harmful to human health and the environment. Therefore, it becomes increasingly important to detect VOC gases in the environment to provide people with a healthy and comfortable living environment.

Over the past few decades, many types of gas sensors have been developed based on different materials and methods. Existing gas sensors include catalytic combustion, electrochemical, thermal conductivity, infrared absorption, paramagnetic, solid electrolyte, and metal oxide semiconductor sensors [1].

The demand for operating temperature becomes more stringent when new materials are employed in gas sensors. In their article, Li *et al.* explore the influence of operating temperature on the response of sensors when using ZnO/Zn2SnO$_4$ composite material as the sensing material. The response of three sensor samples to 100 ppm formaldehyde was recorded at different operating temperatures ranging from 120°C to 230°C. The response of all three sensors increased with rising temperature, reaching a peak at 160°C, and subsequently decreased with further temperature increase. Therefore, it can be inferred that at lower operating temperatures (below 160°C), the reaction between formaldehyde and adsorbed oxygen is accelerated, increasing sensor response. However, with further temperature elevation (above 160°C), the desorption rate of adsorbed oxygen exceeds the adsorption process, leading to a reduction in the mass of adsorbed oxygen and a subsequent decrease in sensor response [2].

Ma *et al.* highlighted in their research on the fabrication of three-dimensional Ce-doped SnO multilevel microspheres and their application in formaldehyde gas sensors that gas sensors based on semiconductor materials exhibit high sensitivity to operating temperature. To determine the optimum operating temperature, the response of sensors based on Sn_3O_4 and Ce-Sn_3O_4 graded microspheres to 100 ppm formaldehyde was evaluated across a range of operating temperatures from 65°C to 325°C. The results demonstrated that the response values of all sensors increased with rising operating temperature, peaking at 200°C, and subsequently decreased with further temperature elevation [3].

Due to the requirement for precise temperature control to ensure excellent material performance, the control of operating temperature in gas sensors is of paramount importance. However, currently available gas monitoring devices on the market, despite their portability, lightweight design, and fast detection speed, generally lack the ability to control the operating temperature of the sensors. Commonly used sensor modules rely on fixed heating resistors and fixed voltage for sensor heating. Additionally, these devices are often constrained by microprocessors and circuitry, and the presence of multiple functionalities tends to reduce the range of detectable gas types [4-7].

In response to the aforementioned issue, the research team embarked on a study and devised a sensor module capable of controlling the heating temperature to a certain extent. This was done to address the varying temperature requirements when applying novel materials to gas sensors. Additionally, based on the sensor module design, a VOC gas monitoring system was developed using an STM32 microprocessor and communicating with up to 16 sensors via the I2C interface.

2. Materials

2.1. Overall system design framework

The VOC monitoring system is mainly divided into roughly four modules. This system comprises temperature and humidity sensors, VOC gas sensors, EC800N-CN Internet of Things (IoT) wireless module, ADS1015 analog-to-digital converter, power supply section, etc. The overall structure of the system is illustrated in **Figure 1**.

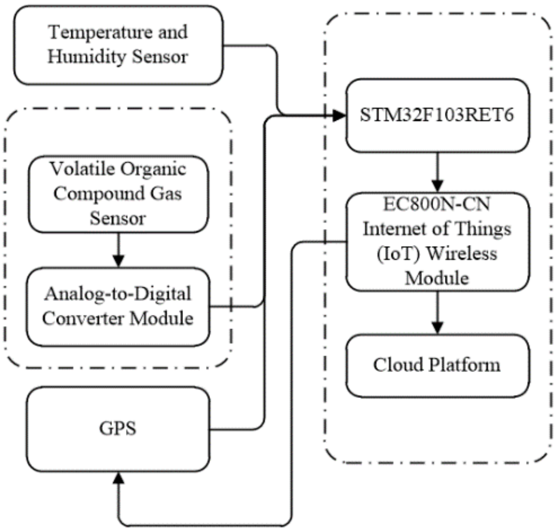

Figure 1. System block diagram

(1) Sensor module: This module is the most important component of the system as it forms the foundation for all the operations [8]. The module is divided into three parts. The first part consists of a matrix composed of 16 gas sensors, which are responsible for collecting information on various harmful gases in the environment and generating analog signals. The second part is the DHT11 temperature and humidity sensor, which outputs a single bus and directly obtains digital signals transmitted to the STM32. The third part is the GPS function in the EC800N-CN module, which transfers the acquired device location information to the STM32.

(2) Data acquisition module: This module is the core of environmental monitoring. Its function is to convert the analog signals from the gas sensor matrix into digital signals and then pass them to the STM32 for further processing. It consists of four ADS1015 converters, which communicate with the STM32 through I2C (serial communication protocol) for data transmission.

(3) Process control and data processing module: This module is the central part of the monitor and performs functions such as data conversion and processing, initialization of various hardware systems, and initialization of the 4G display module.

(4) Data output module: This module is responsible for transmitting real-time monitoring data to the cloud platform via 4G, facilitating data viewing and analysis. It consists of an EC800N-CN module.

2.2. Circuit design

2.2.1. Main control circuit

In this study, the main control chip of the monitoring system adopts the STM32F103RET6 microprocessor launched by STMicroelectronics. Thanks to the powerful control functions of the STM32, using it as the main control chip for the atmospheric VOCs monitoring system is highly appropriate [9].

2.2.2. Power circuit

The STM32 operates within a supply voltage range of 2.0 to 3.6V. In the design of the main control chip power supply section, a unified 3.3V is chosen for this system. Additionally, external ADCs using I2C communication are employed in the system design to collect and convert sensor analog signals [10]. Thus, two separate 3.3V power supplies are required to power the main control unit and the ADCs along with the sensor measurement section. Furthermore, a 5V power supply is needed for the sensor heating section. Therefore, the system design necessitates multiple different voltage levels. In summary, the system design utilizes a common 9V power adapter connected to the 220V AC power supply as the main power source, and alternatively, a 9V battery pack can be used as a power source. The schematic diagrams for the 5V and 3.3V power supply circuits are illustrated in **Figure 2**.

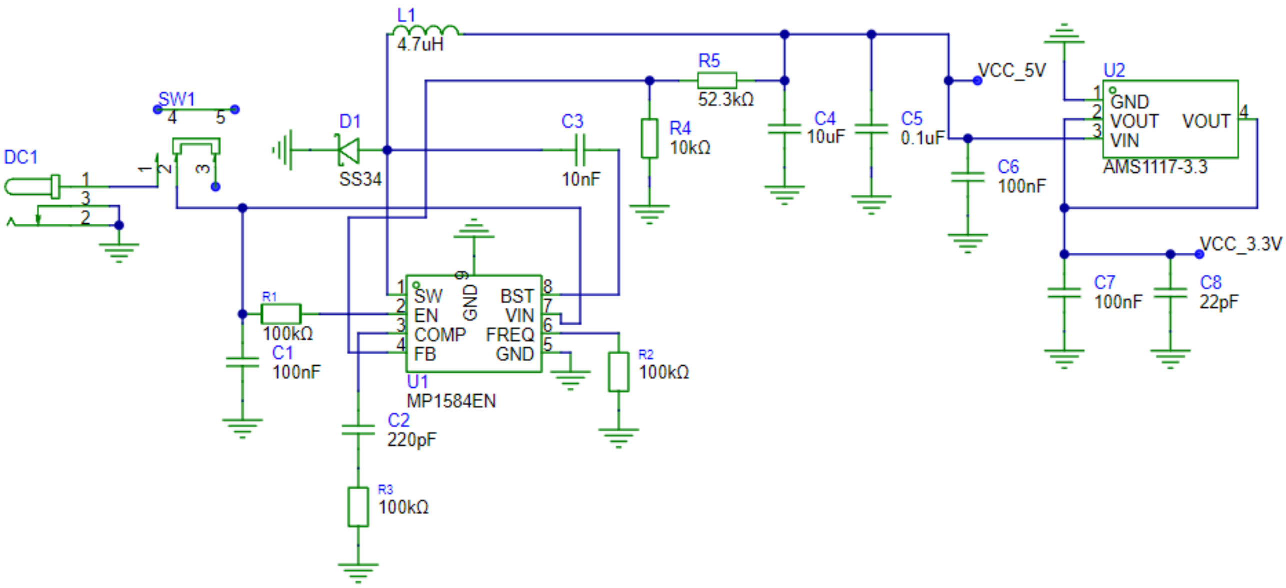

Figure 2. Power circuit schematic diagram

2.2.3. Circuitry for the data acquisition module

The data acquisition is completed using ADS1015, which supports both single-ended and differential measurements, featuring four programmable gain amplifiers with a gain range of +/-2/4/8/16V. The maximum sampling rate can reach 860sps. It converts the collected analog signals into digital ones for STM32 to read and process. The schematic diagram of a single ADC module is shown in **Figure 3**.

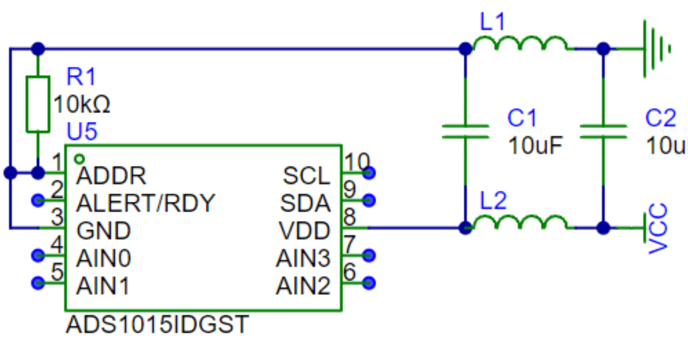

Figure 3. Schematic diagram of individual ADC module circuit

Furthermore, in order to capture a wider range of VOC gases, the monitoring system employs four ADS1015 devices connected in parallel. Each ADS1015 is configured with a unique address, enabling the collection of data from 16 analog signals. The schematic diagram for the parallel connection of the four ADS1015 devices is depicted in **Figure 4**.

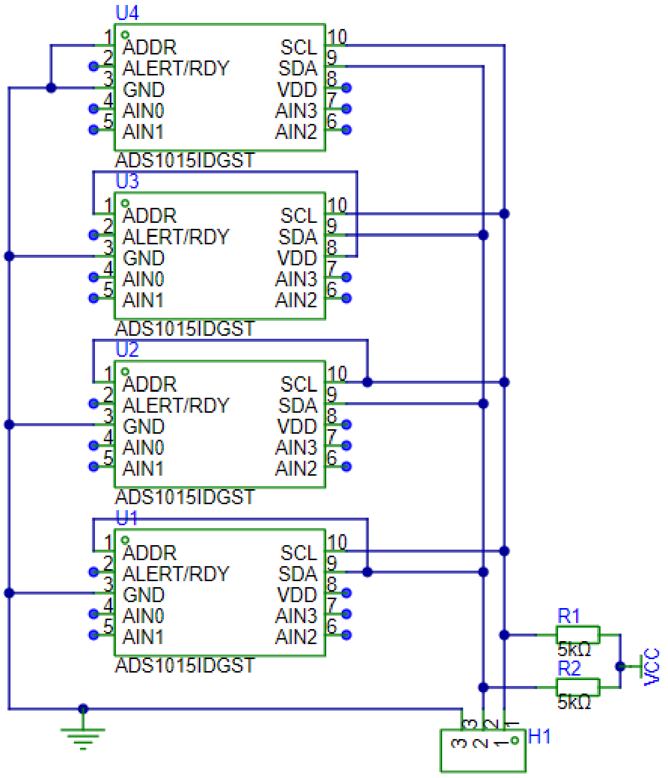

Figure 4. Schematic diagram of parallel connection of four ADS1015

2.2.4. Circuit of VOC gas sensor module

The primary task of this monitoring system is the data acquisition of VOC gases. In this system, the design separates the sensor heating and measurement processes [11]. The measurement component's AO, an analog output signal, connects to the signal receiving pin of the ADS1015, while the heating component utilizes an LM2596-ADJ DC-DC buck converter to adjust the heating voltage. The system is designed to regulate a 5V voltage to meet the heating temperature requirements of different metal oxide materials in the sensors, ensuring optimal operating temperatures for the metal oxide sensors. The circuit schematic of the VOC gas sensor module is shown in **Figure 5**.

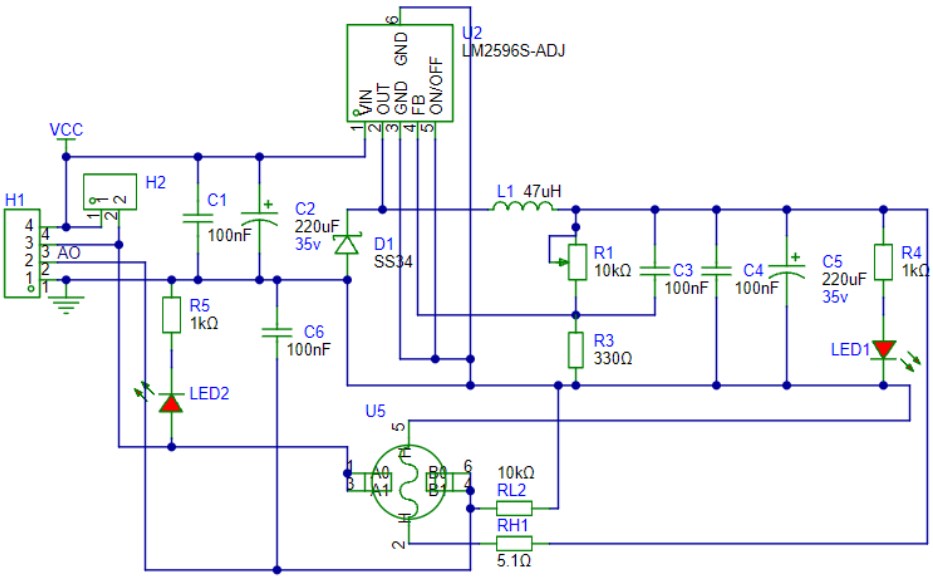

Figure 5. Schematic diagram of VOC gas sensor module circuit

2.2.5. Circuit of 4G module

The 4G functionality of this system is implemented using the EC800N-CN module. By inserting a SIM card into the SIM card interface provided by the EC800N-CN module, the VOC gas data received by STM32 is uploaded to Alibaba Cloud via 4G signals. The circuit schematic of the wireless data communication module is shown in **Figure 6**.

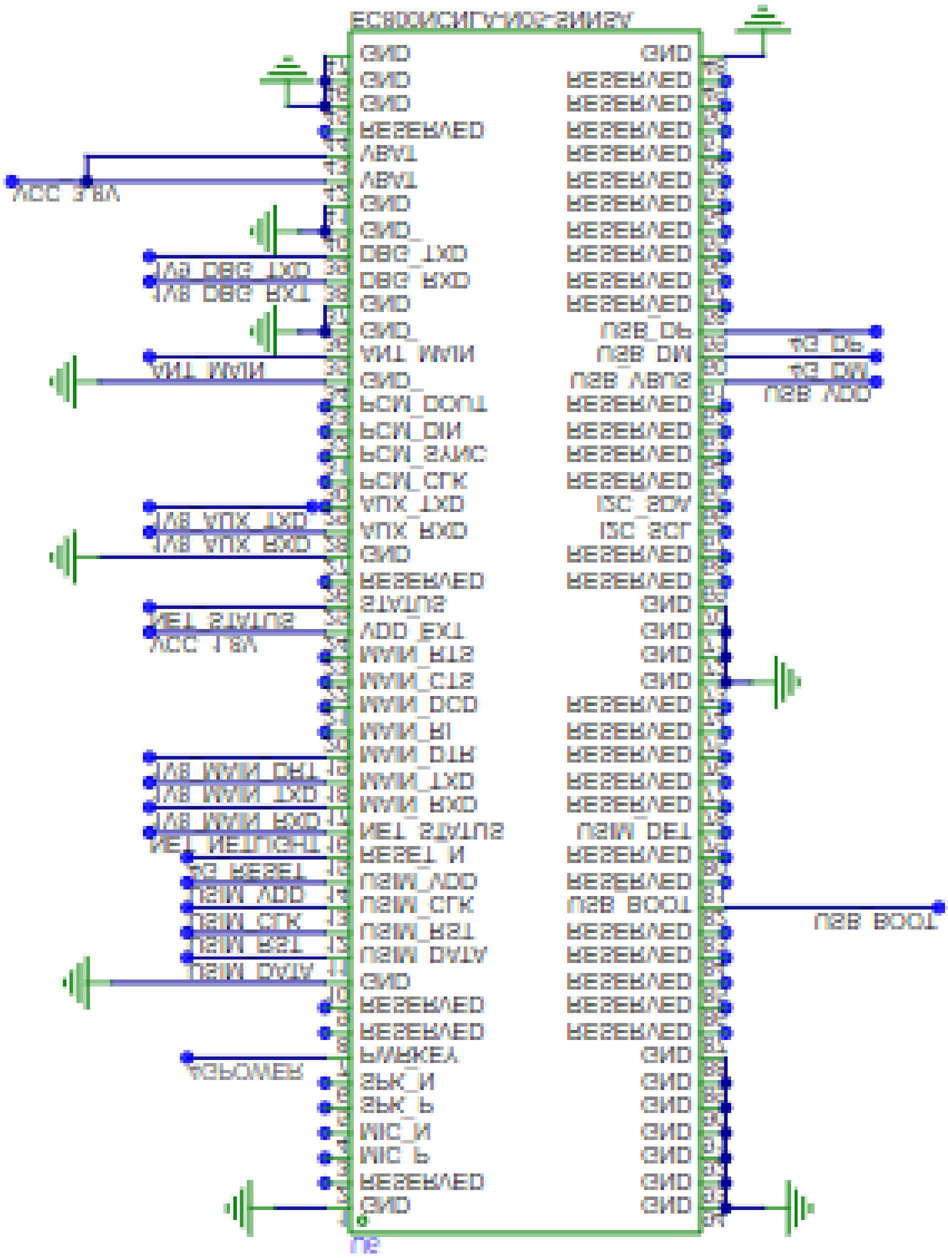

Figure 6. Schematic diagram of wireless data communication module circuit

3. Method

3.1. Development of the main program

The main program primarily facilitates MQTT-based communication between the STM32 and the cloud platform, enabling the collection and transmission of VOC gas concentrations, temperature, humidity, and geographical location data. The first step involves calling the initialization routine, which includes initializing I2C, ADS1015 analog-to-digital conversion (ADC), EC800N-CN module initialization, direct memory access (DMA), serial ports, and real-time clock (RTC). The second step involves self-checking to verify the successful initialization and normal operation of hardware components such as I2C, DHT11, ADS1015, and EC800N-CN, as well as the ability to read and write data through various interfaces. Subsequently, under the control of the clock control system, data is sampled and processed every 10 seconds [12].

3.2. Design of data acquisition program

Based on the I2C bus and ADS1015 (ADC), a program for the ADC module is designed. Initially, the STM32's I2C module is initialized, which includes configuring the GPIO for I2C and setting up the I2C mode. Subsequently, the ADS1015 is initialized, completing its configuration. Upon powering up the STM32 and ADS1015, the STM32 checks for the presence of the ADS1015. Once confirmed, it begins receiving the 12-bit digital signals collected by the ADS1015. These digital signals, when divided by 1000, represent the voltage signal VOUT detected by the VOC module at a certain concentration. Through formula (1), the resistance value RL can be obtained.

$$R_L = \frac{R_{L2} \times (3.3V - V_{OUT})}{V_{OUT}} \tag{1}$$

V_{OUT}: The analog voltage signal output by the circuit

R_L: The resistance value that reflects the change in gas concentration

R_{L2}: The measuring resistance

$3.3V$: The total voltage of the measuring circuit

Once R_L is obtained, the ratio of R_L to the initial resistance R can reflect the gas concentration in the current environment.

3.4. Design of the 4G module program

This monitoring system utilizes the Alibaba Cloud IoT platform as the data receiving end. It achieves data transmission to the cloud by customizing products and devices and creating physical models for display. Moreover, historical information uploaded by devices to the platform is archived for easy access to past data. The STM32 employs the MQTT protocol to transmit data to the cloud via wireless data communication modules. Data intended for transmission is packaged into JSON format [13].

3.5. Standard laboratory equipment

To test the feasibility of the proposed device, data collected by the device was compared with that of standard laboratory equipment. Thus, we also used the CGS-8 Intelligent Gas Sensitive Analysis System (resistive type) as a control group for experimental validation. The physical diagram of the CGS-8 Intelligent Gas Sensitive Analysis System is shown in **Figure 7**.

Figure 7. CGS-8 intelligent gas-sensitive analysis system

The operating temperature of the sensor is controlled by adjusting the magnitude of the heating current. The resistance is tested using the direct current voltage division method. There are 8 independent testing channels, each integrating 6 ranges of load measurement levels. The system automatically selects the appropriate range for testing [14].

4. Results

4.1. Sensor module temperature control effect test

Test the function of adjusting the heating temperature of the sensor module. The actual heating temperature under room temperature conditions was measured using infrared temperature measurement equipment. The data is shown in **Table 1**, including the corresponding heating voltage, the actual measured temperature, and the fitted temperature.

Table 1. Tubular semiconductor with cold-state resistance of 30 ohms for the heating wire

Heating voltage	Actual temperature (℃)	Fitted temperature (℃)
1.74V	84	70.25
2.43V	132	134.71
3V	173	186.28
3.87V	263	272.24
4.89V	367	362.49
6V	464	469.93

4.2. Data transmission effect of the IoT platform

To test the stability of the monitoring system and its sensitivity to VOC gases, the sensor module was connected to the equipment and placed inside a sealed test chamber. Different concentrations of VOC gases were injected incrementally, and the changes in the digital signal received by the system were observed. **Figure 8** shows the temperature and humidity displayed on Alibaba Cloud, as well as the digital data collected by the sensors. These data were updated in real-time and can also be viewed in the log service of the Alibaba Cloud IoT platform to access historical data [15].

Figure 8. Cloud platform receives data

4.3. Test data of different gas concentrations

During the testing of this monitoring system, standard gas sensor probes MQ3, MQ7, MQ8, and the newly tested material probe SnO_2/Zn2SnO_4 were utilized. Significant response curves were obtained for the testing of ethanol with MQ3 and SnO_2/Zn2SnO_4 probes, demonstrating excellent sensitivity. The graphs illustrate that the AD values collected by each probe rapidly increase upon sample insertion, reaching stability around 30 seconds. This is because it takes time for the liquid sample to diffuse throughout the entire space after being dripped in, and the AD values quickly return to their initial values after the isolation hood is opened. **Figure 9** depicts the response testing of ethanol using the MQ-3 sensor probe and the SnO_2/Zn2SnO_4 probe, with different concentrations of ethanol injected and the corresponding digital signal values received by the cloud platform.

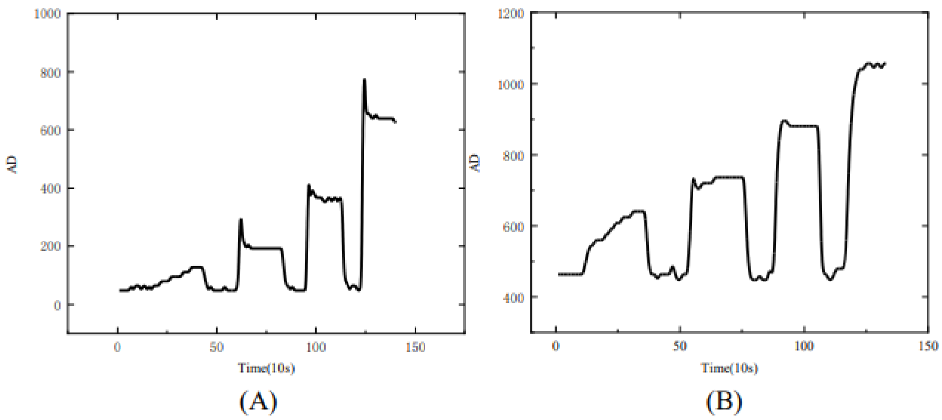

Figure 9. Response curves of MQ-3 and SnO_2/Zn_2SnO_4 to ethanol

After conducting tests with different concentrations of acetone for MQ7, MQ8, and SnO_2/Zn2SnO_4, as well as tests with different concentrations of ethanol for MQ, sensitivity curves for several probes were obtained.

Furthermore, sensitivity curves for the same four probes under identical conditions were obtained using the experimental equipment CGS-8. **Figure 10** illustrates sensitivity value curves obtained using two devices for (A) MQ7, (B) MQ8, (C) SnO_2/Zn2SnO_4, and (D) MQ-3, respectively.

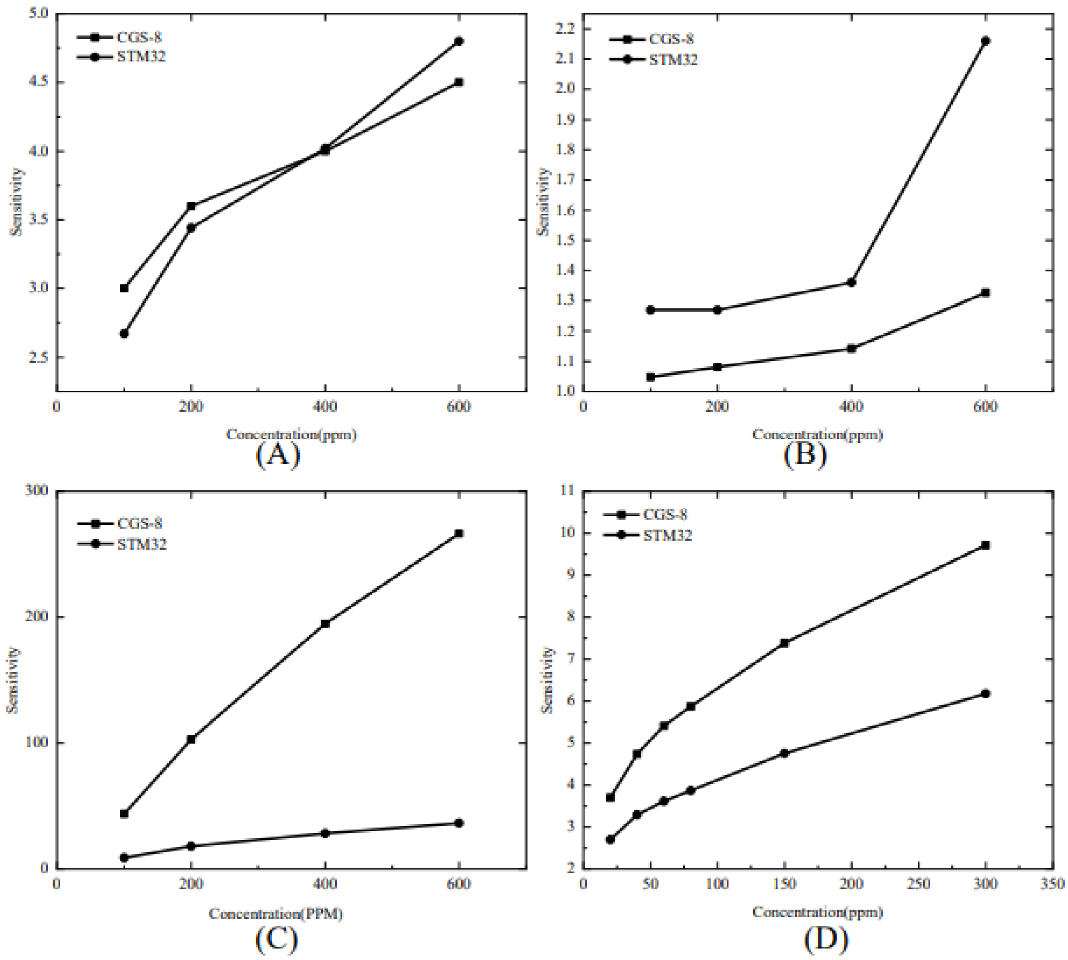

Figure 10. Relationship curve between sensitivity and concentration

5. Conclusion

Experimental validation of the IoT-based VOC sensing system developed by the research team demonstrates that the system can upload collected data to IoT platforms via 4G, and can perform gas testing with different material sensors. After successfully controlling the working temperature of the sensors and comparing the results with professional equipment under equivalent conditions, the system can reliably and accurately collect gas concentration information. Thus, the system features high precision, fast data upload times, and compatibility with various material sensors. In most cases, the sensitivity of the detection system to gases is comparable to that of professional equipment. Sensitivity curves for MQ7, MQ8, and SnO_2/Zn2SnO_4 material probes testing different concentrations of acetone were obtained using both the designed equipment and the professional testing device CGS-8. The sensitivity error of the MQ7 probe points is relatively small, with a maximum error of 10% and a minimum error of 0.5%, with an average error of 5.6%. Although there is a significant difference in sensitivity data between the two devices for MQ8 and SnO_2/Zn2SnO_4 material probes, both demonstrate sensitivity to acetone, showing similar overall trends and high sensitivity. As noted in other literature, the response of metal oxide-type sensors can be influenced by local temperature and humidity levels. Therefore, signal fluctuations may occur due to environmental temperature and humidity, affecting data reliability. However, the system possesses certain environmental detection capabilities and can compensate for influencing factors through environmental factor analysis and algorithm implementation in the program in subsequent stages.

Disclosure statement

The authors declare no conflict of interest.

References

[1] Dey A, 2018, Semiconductor Metal Oxide Gas Sensors: A Review. Mater. Sci. Eng. B. 229: 206–217.

[2] Li X, Zhang N, Liu C, et al., 2021, Enhanced Gas Sensing Properties for Formaldehyde Based on ZnO/Zn2SnO4 Composites from One-Step Hydrothermal Synthesis. Journal of Alloys and Compounds, 850: 156606.

[3] Ma X, Shen J, Hu D, et al., 2017, Preparation of Three-Dimensional Ce-doped Sn3O4 Hierarchical Microsphere and its Application on Formaldehyde Gas Sensor. Journal of Alloys and Compounds, 726: 1092–1100.

[4] Aghili NS, Rasekh M, Karami H, et al., 2023, Aromatic Fingerprints: VOC Analysis with E-Nose and GC-MS for Rapid Detection of Adulteration in Sesame Oil. Sensors 23: 6294. https://doi.org/10.3390/s23146294

[5] Sharma C, Dey A, Khatun H, et al., 2023, Design and Development of a Gas Sensor Array to Detect Salinity Stress in Khasi Mandarin Orange Plants. IEEE Transactions on Instrumentation and Measurement, 72: 1–9.

[6] Linto Sibi SP, Rajkumar M, Govindharaj K, et al., 2023, Electronic Sensitization Enhanced p-Type Ammonia Gas Sensing of Zinc Doped MoS2/RGO Composites. Analytica Chimica Acta, 1248: 340932.

[7] Shin W, Hong S, Jeong Y, et al., 2023, Low-Frequency Noise in Gas Sensors: A Review. Sensors and Actuators B: Chemical, 383: 133551.

[8] Abdul RN, Ammar Z, Nora J, et al., 2017, Applications of Sensing Material on Quartz Crystal Microbalance in Detection of Volatile Organic Compounds: A Review. Glob. J. Eng. Technol. Rev. 2: 10–22.

[9] Molla Abbasi P, 2021, Organic Compound Gas Detector Based on Polylactic Acid/Poly (Styrene-Co-Acrylonitrile)/ Multi-Walled Carbon Nanotube Blend Composite with Co-Continuous Microstructure. Polymers for Advanced Technologies, 33(3): 112–113.

[10] Shurmer HV, Gardner JW, 1992, Odour Discrimination with an Electronic Nose. Sens. Actuators B Chem. 8: 1–11.

[11] Sun YF, Liu SB, Meng FL., et al., 2012, Metal Oxide Nanostructures and their Gas Sensing Properties: A Review. Sensors,12: 2610–2631.

[12] Tang KT, Chiu SW, Pan CH, et al., 2010, Development of a Portable Electronic Nose System for the Detection and Classification of Fruity Odors. Sensors (Switzerland), 10: 9179–9193.

[13] Wilson AD, Baietto M, 2011, Advances in electronic-nose technologies developed for biomedical applications. Sensors, 11: 1105–1176.

[14] Wilson AD, Baietto M, 2009, Applications and Advances in Electronic-Nose Technologies. Sensors, 9: 5099–5148.

[15] Zampolli S, Elmi I, Stürmann J, et al., 2005, Selectivity Enhancement of Metal Oxide Gas Sensors Using a Micromachined Gas Chromatographic Column. Sens. Actuators B Chem. 105: 400–406.